Outage Probability Analysis of the Protected Tactical Waveform (PTW) on the Return Link

Lan K. Nguyen*, Richard B. Wells[b], Duy H. N. Nguyen‡, Nghi H. Tran†
*LinQuest Corp, Los Angeles, CA
[b]Dept. of Electrical Engineering, University of Idaho, Moscow, ID
‡Dept. of Electrical Engineering, San Diego State University, San Diego, CA
† Dept. of Electrical Engineering, University of Akron, Akron, OH

Abstract — **This paper analyzes the outage probability of a multicarrier signal, using the Protected Tactical Waveform (PTW) on the return link (RL). The signal is relayed over a nonlinear distorted satellite transponder. The transponder is modelled to include a gain element, a soft limiter, and a travelling wave tube amplifier (TWTA); a Shaleh model is used to model the TWTA. The outage probability is determined when the probability of the mutual information random variable is less than the code rate. The outage probability is used as a theoretical bound for maximum capacity. This bound serves as an important benchmark of the achievable rate for the RL. The degree in which M-ary phased shift keying (MPSK) signals using Digital Video Broadcasting – Satellite – Second generation (DVB-S2) forward error correction (FEC) with numerous code rates to achieve this bound is investigated by computer simulation, and also discussed in the paper.**

Keywords — ***Transponder; Nonlinearity; Multicarrier; Protected Tactical Waveform; DVB-S2; Outage Probability.***

I. INTRODUCTION

Satellite communications (SATCOM) systems of the future face challenges from on-going advances in technology, expanding mission scope, increasing data rate requirements, and evolving threat ennvironments. The future capacity of the Military Satellite communications (MILSATCOM) is projected to surpass current demand and to increase many-fold in contested environment [1]. To address this challenge, meeting high capacity for protected communication service, and provide low-cost solutions, the Air Force is planning to demonstrate its newly developed protected tactical waveform (PTW) over multiple frequency bands. The PTW is designed to support wideband protected communication services against numerous jamming threats [2]. High capacity is achieved based on the latest modulation and coding techniques to deliver performance that approaches to the theoretical Shannon limit [3]. Protected communication service is achieved based on frequency diversity, time diversity, and powerful forward error correction (FEC) coding. Frequency diversity is achieved by frequency hopping spread spectrum (FHSS) technique; time diversity is achieved by TRANSEC driven time randomization and interleavers; and FEC is performed by Digital Video Broadcasting – Satellite – Second generation (DVB-S2) FEC [4]. This powerful FEC is based on the concatenation of of BCH (Bose-Chaudhuri-Hocquengham) and LDPC (Low Density Parity Check) codes. Finally, affordability is based on the existence of satellites with terminal upgrades to support wideband communication services. In addition, new upgrades are levied on the availability and the maturity of the DVB-S2 standard. DVB-S2 is widely used in comercial television and data broadcasting services, its technology is mature, and its performance is also widely known.

A satellite network is typically comprised of the space segment, the ground segment, and the terresterial networks that interface with the ground segment. The space segment acts as a transmission relay; it is comprised of the satellites. The ground segment is comprised of the users and the Hub, the system controller (SC). TRANSEC keys are distributed by the Hub to its members to ensure the hopping signals do not overlap each other's bandwidth. A traveling wave tube amplifier (TWTA) is a high gain, low noise, wide bandwidth microwave amplifier. It provides significant high power output and effiencies. It is capable of gains on the order of 40-50 dB [5]. For these reasons, TWTA is commonly used in satellite communication and is the primary amplification element of the transponder. TWTA is also the largest contributor to transmission nonlinearities. A multicarrier signal typical exhibits high Peak-to-Average power Ratio (PAR). When this signal passes through a nonlinear TWTA, nonlinear distortions occur and intermodulation (IM) [6 - 9] products are generated, which result in spectral regrowth. In nominal operation, input power is backed off (IBO) so that the TWTA is operating in the linear region. In addition, the TWTA is often protected by another nonlinear device, a soft limiter which prevents the signal running into the saturation region, causing thermal instability which can damage the TWTA. In this study, a Shaleh model [10] is used for the TWTA. To simplify the simulation and the anlysis, in this paper, an automactic gain control (AGC), a soft limitter, and a TWTA are used to model the transponder. The AGC is adjusted on a hop-to-hop basis so that the average input signal power to the TWTA is at the desired operating point.

Early development of information theory suggests that mutual information can be defined as a random variable [11 - 15] and if the channel behaves egordically, the channel capacity is the largest rate at which the information is transmitted [16], provided the blocklength is allowed to grow without bound. To this end, the bound for achievable rate is of great interests for finite blocklength codes. The exact bound for short length codes, n as short as 100, is discussed in [17]. For moderate length codes, $n > 1000$, the bound can be characterized in terms of outage probability [18]. The outage probability is determined when the mutual information random variable is less than the code rate. The outage probability is used as a theortical bound and shown to be a good performance metric for predicting the

978-1-5386-0595-0/17/$31.00 ©2017 IEEE

Authorized licensed use limited to: Georgia Institute of Technology. Downloaded on January 12,2023 at 20:50:38 UTC from IEEE Xplore. Restrictions apply.

achievable rate. Motivated by this perspective, this paper examines the outage probability of the M-ary phased shift keying (MPSK) using DVB-S2 FEC, with numrous code rates, for a fixed code length of 16,200 coded bits, that support PTW over a nonlinear satellite transponder. How close to this bound for MPSK signals combined with DVB-S2 FEC do come, is discussed in the paper.

There are two links for the transponding satellite systems. The RL is the communication connection initiated by the user to the transponder and terminated at the ground hub SC terminal. The forward link (FL) is the reversed link. This paper addresses the RL, the results of this paper can be readily extended to the FL. A notional block diagram of a beam for the RL is shown in Fig. 1.

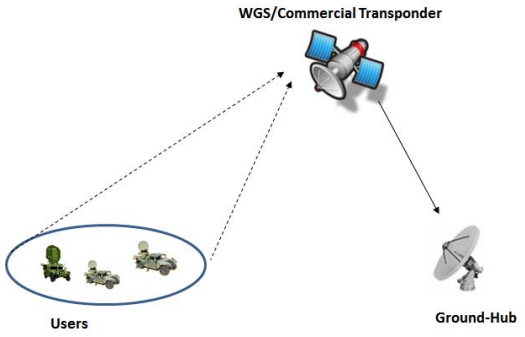

Fig. 1. Notional RL block diagram.

II. SYSTEM MODEL

Without loss of generality, baseband signaling is considered. At the input of the transponder, the multicarrier signal is given by

$$x_M(t) = x(t) + \sum_{m=1}^{N} x_{aci}(t,m) + n_{ul}(t) \quad (1)$$

where $x(\cdot)$ denotes signal of interest (SOI), $x_{aci}(\cdot)$ denotes adjacent channel interference (ACI) signal, N denotes number of adjacent channels in a channel group, and $n_{ul}(\cdot)$ denotes uplink (UL) channel noise, complex-value additive white Gaussian noise (AWGN), with two-sided power spectrum density N_o.

Signal of interest is given by

$$x(t) = \sum_{\mathrm{n}} A \mathrm{d}_{\mathrm{n}} g_i(t - \mathrm{n}T_i), \quad (2)$$

where A denotes signal amplitude, $\{d_n\}$ denotes transmitted symbols from the MPSK alphabet, T_i denotes the symbol period, $g_i(\cdot)$ denotes the spectral shaping filter. In this paper, the spectral shaping filter is a square root raised cosine (SRRC) filter with a roll-off factor $\beta = 0.2$.

The end-to-end top level simulation block diagram for the RL is shown in Fig. 2. At the input, messages of information bits entering the DVB-S2 encoder. The M-ary Phase Shift Keying (MPSK) modulator takes the coded bits and then maps them to form Gray-coded MPSK symbols. The MPSK modulated symbols enter the channel interleaver and are grouped into equal length sequences which form the hops. Reference symbols are then added to each hop. Each hop is then transmitted at a different frequency. Reference symbols and the distribution of reference symbols are known a priori at the ground hub receiver; data symbols contain the information bits. This process is identical for ACI channels. However, ACI signals come from different users, may occupy different bandwidths, different modulations, due to different paths, they arrive to the PL at different times, and therefore ACI signals are completely independent of SOI signal. At the input of the transponder, the aggregated input signal includes SOI, ACI signals, and UL noise. The transponder relays the signal on the downlink (DL). The performance impact due to transponder nonlinearities and noise power robbing are exhibited on the downlink. At the ground hub receiver, received signal is de-interleaved, demodulated, and decoded by the DVB-S2 decoder. Decoded messages are then compared with transmitted messages to determine the block error rate (BLER).

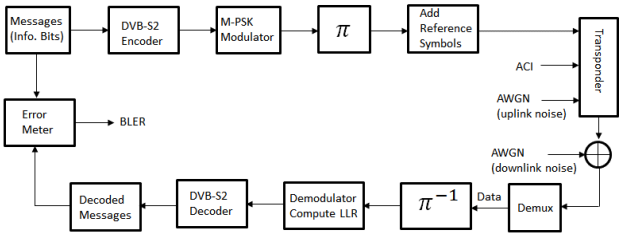

Fig. 2. RL end-to-end block diagram.

The channel spacing between two signals is given by

$$\Delta f_i = 1.33 \left(\frac{R_i + R_{i+1}}{2}\right) \quad (3)$$

where R_i and R_{i+1} denote the symbol rates of the ith and (i+1)th users, respectively. Symbol rate of the ith user is given by

$$R_i = \frac{1}{T_i}. \quad (4)$$

A. *Transponder Model*

In this paper, the transponder consists of an automatic gain control (AGC), a soft limiter, and a TWTA. The AGC is adjustable on a hop-by-hop basis. This AGC is used to ensure the TWTA operates in the linear region. The primary purpose of a soft limiter is to limit the signal running into the saturation region of the TWTA. The instantaneous nonlinear characteristics of the soft limiter is given as

$$S_L(x_L) = \begin{cases} x_L, & |x_L| \le R \\ Re^{iarg(x_L)} & |x_L| > R \end{cases}, \quad (5)$$

Authorized licensed use limited to: Georgia Institute of Technology. Downloaded on January 12,2023 at 20:50:38 UTC from IEEE Xplore. Restrictions apply.

The block diagram of a simplified transponder is shown in Fig. 3.

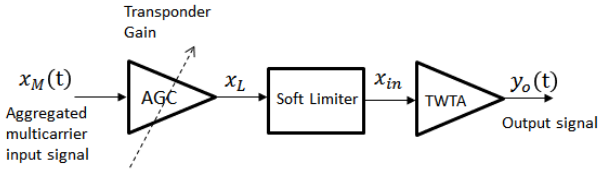

Fig. 3. Simplified transponder block diagram.

B. Transponder TWTA

A Shaleh model for nonlinear amplitude and phase distortions is assumed for the TWTA. The two-parameter formulas that represent the amplitude and phase distortions are given by [10]

$$A(r) = \frac{\alpha_a r}{1+\beta_a r^2} \qquad (AM-AM) \tag{6}$$

$$\Phi(r) = \frac{\alpha_\varphi r^2}{1+\beta_\varphi r^2} \qquad (AM-PM) \tag{7}$$

where

$$\alpha_a = 2,\ \beta_a = 1,\ \alpha_\varphi = 4,\ \beta_\varphi = 9.1, \tag{8}$$

and r denotes the instantaneous magnitude of the signal. To simplify the analysis, the above AM-AM distortion parameters are chosen so that the peak is at unity. The magnitude and phase characteristics of the TWTA are shown in Fig. 4.

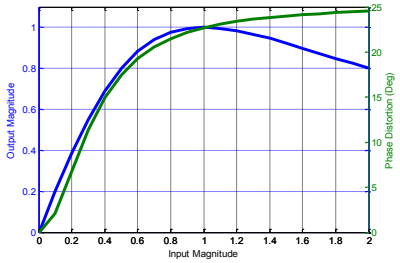

Fig. 4. TWTA AM-AM and AM-PM characteristics.

In general, the output signal of the TWTA is given by

$$y_o(t) = \alpha x_{in}(t) + n_{IM}(t) \tag{9}$$

where α denotes linear gain or undistorted gain, $n_{IM}(\cdot)$ denotes intermodulated noise with noise density IM_o, assumed to be AWGN, and the level of the intermodulated noise is a function of the operating point of the TWTA, and $x_{in}(\cdot)$ and $y_o(\cdot)$ denote input and output multicarrier signals of the TWTA, respectively.

At the input of the TWTA, the signal is Gaussian, the magnitude $r(t)$ has a Rayleigh distribution with a density function given by

$$f(r;\sigma_r) = \frac{re^{\frac{-r^2}{2\sigma_r^2}}}{\sigma_r^2}, \quad r \geq 0. \tag{10}$$

Applying Bussgang theorem [19], undistorted signal gain is given by

$$\alpha = \frac{E\{rA(r)\}}{2\sigma_r^2} \tag{11}$$

where $E\{\cdot\}$ denotes the expectation operator, and $A(r)$ is given by (6). Furthermore,

$$\sigma_r^2 = \frac{P_{in}}{2} \tag{12}$$

where P_{in} denotes input signal power to the TWTA. Using (10), (11) and (12), and solving for undistorted signal gain, with the help of [20], one obtains

$$\alpha = \frac{2}{P_{in}} + \frac{2}{P_{in}^2} e^{\frac{1}{P_{in}}} Ei\left(\frac{-1}{P_{in}}\right) \tag{13}$$

where

$$\mathrm{Ei}(x) = \int_{-\infty}^{x} \frac{e^t}{t} dt. \tag{14}$$

C. Transponded Mutual Information

Undistorted signal gain is applied to both uplink signal and noise. Without loss of generality and to simplify the analysis, undistorted signal gain is normalized at unity, and for brevity, the transponder output signal for the channel of interest is given by

$$y(t) = x(t) + n(t) \tag{15}$$

where the aggregated noise is given by

$$n(t) = n_{ul}(t) + n_{aci}(t) + n_{IM}(t), \tag{16}$$

where $n_{aci}(\cdot)$ denotes the equivalent ACI noise, assumed to be AWGN, with noise density I_o. The mutual information between the input and output signals of the transponder is given by

$$i(x;y) = log\left[\frac{f_{Y|X}(y|x)}{f_Y(y)}\right] \tag{17}$$

where $log(\cdot)$ denotes the natural logarithmic function, $f_{Y|X}(y|x)$ denotes the conditional probability density function (pdf) of random variable Y given random variable X. In this paper, Input MPSK signal is also assumed to be Gaussian distributed. Under Gaussian distributions assumption of the input and output signals and noise, the conditional pdf of random variable Y given random variable X is given by

Authorized licensed use limited to: Georgia Institute of Technology. Downloaded on January 12,2023 at 20:50:38 UTC from IEEE Xplore. Restrictions apply.

$$f_{Y|X}(y|x) = \frac{1}{\pi(N_o+I_o+IM_o)} exp\left(-\frac{|y-x|^2}{N_o+I_o+IM_o}\right), \quad (18)$$

and the pdf of the output signal is given by

$$f_Y(y) = \frac{1}{\pi(E_s+N_o+I_o+IM_o)} exp\left(-\frac{|y|^2}{E_s+N_o+I_o+IM_o}\right) \quad (19)$$

where E_s denotes symbol energy. Substituting (18) and (19) into (17); the mutual information is given by

$$i(x;y) = log\left(1+\frac{E_s}{N_o+I_o+IM_o}\right) + \frac{|y|^2}{E_s+N_o+I_o+IM_o} - \frac{|y-x|^2}{N_o+I_o+IM_o}. \quad (20)$$

Again, E_s denotes symbol energy, N_o, I_o, and IM_o denote UL noise density, ACI noise density, and intermodulated noise density, respectively, input signal $x(\cdot)$ is given by (2) and output signal $y(\cdot)$ is given by (15). The average mutual information is given by

$$I(X;Y) = E\{i(x;y)\} = log\left(1+\frac{E_s}{N_o+I_o+IM_o}\right), \quad (21)$$

The average mutual information (21) can also be expressed as

$$I(X;Y) = \lim_{m\to\infty} \frac{1}{m}\sum_{k=1}^{m} i(x_k;y_k). \quad (22)$$

D. *The Outage Probability for Codewords of Finite Length*

The above expression suggests that the average mutual information can be computed based on the mutual information of the input and output vectors of length m [15] i.e.

$$\frac{1}{m} i(x^m;y^m) = \frac{1}{m}\sum_{k=1}^{m} i(x_k;y_k), \quad (23)$$

where m denotes the number of symbols per code word. The expression on the right hand side (RHS) of (23) is also known as the mutual information rate. Given (20) and (23), the mutual information rate can be shown to have the same distribution as random variable Z_m; it is given by

$$Z_m = log\left(1+\frac{E_s}{N_o+I_o+IM_o}\right) + W_m \quad (24)$$

where

$$W_m = \frac{1}{m}\sum_{k=1}^{m}\left(\frac{|Y_k|^2}{E_s+N_o+I_o+IM_o} - \frac{|N_k|^2}{N_o+I_o+IM_o}\right). \quad (25)$$

$|Y|^2$ and $|N|^2$ are chi-square distributed random variables. For 2 degrees of freedom (complex data), chi-square distribution becomes exponential distribution. Furthermore, for $m = 1$, the difference of 2 exponential distributed random variables is a Laplacian random variable. In this case, W_m is a Laplacian random variable with zero mean and variance

$$\sigma_W^2 = \frac{2E_s}{E_s+N_o+I_o+IM_o}. \quad (26)$$

Using Central Limit Theorem, for large m (> 100), W_m is approximated by a Gaussian random variable. The distribution of the Z_m can be approximated as

$$Z_m \sim \mathcal{N}\left(log\left(1+\frac{E_s}{N_o+I_o+IM_o}\right), \frac{2E_s}{m(E_s+N_o+I_o+IM_o)}\right). \quad (27)$$

The cumulative distribution function (cdf) of Gaussian random variable Z_m is given by

$$F_{Z_m}(z) = Q\left(\frac{log\left(1+\frac{E_s}{N_o+I_o+IM_o}\right)-z}{\sqrt{\frac{2E_s}{m(E_s+N_o+I_o+IM_o)}}}\right), \quad (28)$$

or

$$F_{Z_m}(z) = Q\left(\frac{log\left(1+\frac{1}{SNR^{-1}\left(1+\frac{I_o}{N_o}\right)+NPR^{-1}}\right)-z}{\sqrt{\frac{2}{m\left(1+SNR^{-1}\left(1+\frac{I_o}{N_o}\right)+NPR^{-1}\right)}}}\right) \quad (29)$$

where

$$Q(x) = \frac{1}{\sqrt{2\pi}}\int_x^\infty exp\left(-\frac{t^2}{2}\right)dt, \quad (30)$$

$$SNR = \frac{E_s}{N_o}, \quad (31)$$

and intermodulated noise power ratio (NPR)

$$NPR = \frac{E_s}{IM_o}. \quad (32)$$

NPR is a figure of merit for intermodulated distortion caused by a large number of carriers passing through a nonlinear power amplifier. NPR provides an average value effect. When the power spectrum density distribution of the carriers is not uniform, small signal suffers 6 dB of compression. Interested reader is referred to [21] for more details. For a nonlinear amplifier to operate in the linear region, NPR is typically in the range of 16 dB or higher. In this paper, NPR = 16 dB, an input back-off (IBO) of 7 dB, is used in the simulation section of the paper.

Define code rate $R_c \triangleq^{\text{def}} k/n$, where k denotes the number of information bits and n denotes the number of coded bits generated by the DVB-S2 encoder. R_c is typically specified in communications systems. Let R_s denotes the code rate in bits per symbol. R_s is given by

$$R_s = R_c \frac{\#coded\ bits}{symbol}. \quad (33)$$

For QPSK, there are 2 coded bits per symbol; if $R_c = \frac{1}{2}$ then $R_s = 1$. In addition, since natural logarithmic function is used

Authorized licensed use limited to: Georgia Institute of Technology. Downloaded on January 12,2023 at 20:50:38 UTC from IEEE Xplore. Restrictions apply.

to express the mutual information, the code rate should be converted to units of nats per symbol, i.e., $R_e = log(2)R_s$.

When the mutual information rate is less than the code rate R_e, an outage occurs. The probability outage for Z_m is given by

$$P_o = P[Z_m \leq R_e] = F_{Z_m}(R_e), \tag{34}$$

or

$$P_o = Q\left(\frac{log\left(1+\frac{1}{SNR^{-1}\left(1+\frac{I_O}{N_O}\right)+NPR^{-1}}\right)-R_e}{\sqrt{\frac{2}{m\left(1+SNR^{-1}\left(1+\frac{I_O}{N_O}\right)+NPR^{-1}\right)}}}\right). \tag{35}$$

As shown in (35), for large codeword, the outage probability P_o provides a theoretical bound for block error rate (BLER) i.e.

$$BLER \geq P_o. \tag{36}$$

The above bound was derived based on the Gaussian distributions assumption of the signal and aggregated noise, and the average mutual information for codeword of length m. The performance of the MPSK signals using DVB-S2 codes and the bound are discussed subsequently in the simulation results section.

III. SIMULATION RESULTS

Computer simulations for Quadrature Phase Shift Keying (QPSK) and 8 Phase Shift Keying (8PSK), using DVB-S2 FEC with a fixed length of 16,200 coded bits, code rates R_c of 1/4, 1/3, 1/2, 2/3, 3/4 and 8/9 are considered. Details information of the DVB-S2 FEC and the constellations of QPSK and 8PSK are defined in [4]. The transponder is assumed to operate under automatic gain control mode in the linear region, NPR = 16 dB. The transponder is loaded such that the equivalent ACI noise density over noise density $\frac{I_O}{N_O} = -16\ dB$. Perfect channel information on SNR is assumed. A notional power spectrum of the channel group is shown in Fig. 5. In this scenario, the SOI is in the middle of the channel group.

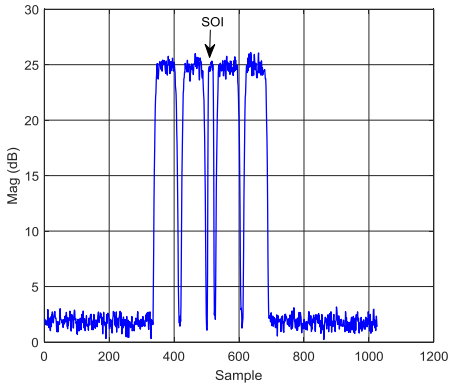

Fig. 5. Power spectrum of the users in a channel group.

Using (35), the outage probability P_o, and the simulated BLER as a function of signal to noise ratio (SNR) for QPSK with code rates $R_c = \left\{\frac{1}{4}, \frac{1}{3}, \frac{1}{2}, \frac{2}{3}\right\}$ are shown in Fig. 6.

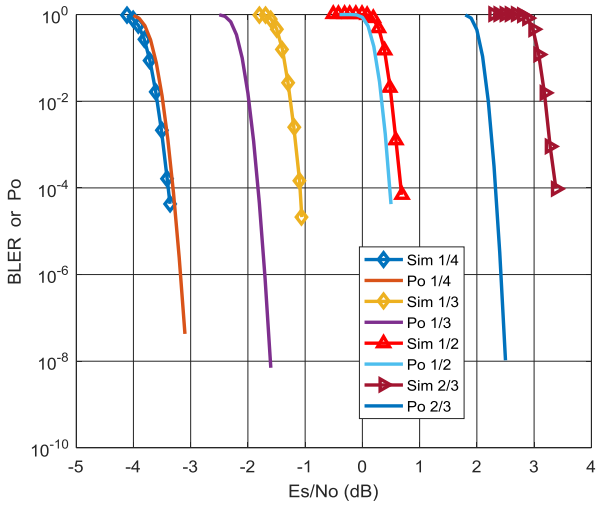

Fig. 6. BLER or Po for QPSK, code rate $R_c = \{\frac{1}{4}, \frac{1}{3}, \frac{1}{2}, \frac{2}{3}\}$.

As discussed in previous section, in general, the outage probability P_o is served as the performance bound. As shown in Fig. 6, the performance of this bound appears to be independent of the code rates. At BLER of 10^{-4}, results shown in Fig. 6 indicate that the difference is

- less than 0.1 dB for code rate 1/4,
- about 0.6 dB for code rate 1/3,
- less than 0.2 dB for code rate 1/2,
- about 1 dB for code rate 2/3.

The BLER and the outage probability P_o for 8PSK with code rates $R_c = \left\{\frac{3}{4}, \frac{8}{9}\right\}$ as a function of SNR are shown in Fig. 7.

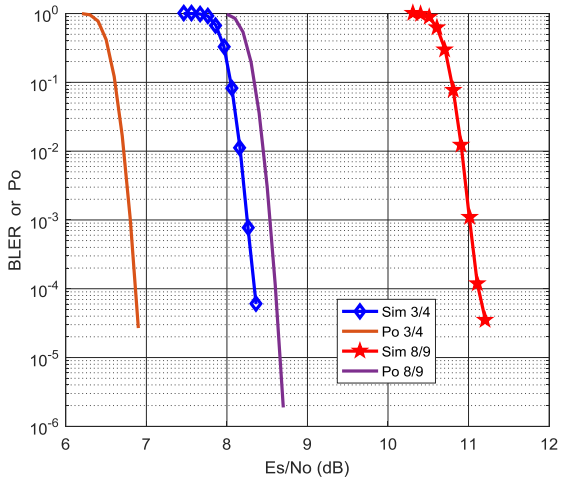

Fig. 7. BLER or Po for 8PSK, code rate $R_c = \{\frac{3}{4}, \frac{8}{9}\}$.

Authorized licensed use limited to: Georgia Institute of Technology. Downloaded on January 12,2023 at 20:50:38 UTC from IEEE Xplore. Restrictions apply.

With a combination of higher order of modulation and code rates, results shown in Fig. 7 indicate that the difference between the outage probability and the simulated BLER is large. For high code rate $R_c = \frac{8}{9}$, at BLER of 10^{-4}, the difference is up to 2.5 dB.

As we discussed in previous section, the outage probability was derived based on the Gaussian distributions assumption of the signal and aggregated noise combined with the decoder performance of DVB-S2 FEC. This assumption is harder to meet for 8PSK and high code rates (higher than 3/4). As a result, the gaps between the theoretical bounds, the outage probabilities, and the performance curves widen as shown in Figure 7.

IV. CONCLUSION

In this paper we used a simple model to represent a nonlinear transponder. The transponder model consists of an automatic gain control element, a soft limiter, and a TWTA. A Shaleh model is used for the TWTA. The transponder is operated in the linear region. Using this transponder model, the performance of the PTW using DVB-S2 FEC with a fixed length of 16,200 coded bits on the RL is characterized. Computer simulation, using QPSK and 8PSK with code rates of 1/4, 1/3, 1/2, 2/3, 3/4, and 8/9 were presented. Under Gaussian distributions assumption of the signal and the aggregated noise, the outage probability for the DVB-S2 FEC was derived. This outage probability can be served as an important bench mark of the achievable rate for PTW. In this study, target BLER of 10^{-4} is considered. For low order of modulation (QPSK) and low code rates of 1/4, this bound can be achieved within 0.1 dB. For high order of modulation (8PSK) and high code rate of 8/9, the Gaussian distributions assumption for the signal and noise combined with the DVB-S2 FEC performance become weak. The system does not achieve this bound and the gap is widen up to 2.5 dB. Disparity between the theoretical limit calculations and actual performance as a function of the higher order modulations is due to assumptions going into the derivation of channel capacity formulas. In particular, the Gaussian assumptions employed here are approximations for which the accuracy is a function of the signaling alphabet. In order to reduce these disparities a more general capacity formula is required [16]. This is the topic of our future research.

REFERENCES

[1] Sullivan, J.; Glaser, M.; Walsh, C.; Dallas, W.; Blackman, J., VanderVennet, J; Shunshine, C.; Chuang, J. C., "Protected Tactical MILSATCOM Design for Affordability Risk Reduction (DFARR) Results," IEEE MILCOM Proceedings, 2014.

[2] Wolf, B. J.; Huang, J. C., "Implementation and Testing of the Protected Tactical Waveform (PTW)," IEEE MILCOM Proceedings, 2015.

[3] Shannon, C. E., "Probability of Error for Optimal Codes in A Gassian Channel," Bell Syst. Tech. J., vol. 38, pp. 611-656, 1959.

[4] ETSI EN 302 307 v1.2.1 (2009-08): Digital Video Broadcasting (DVB), Second generation framing structure, channel coding and modulation systems for Broadcasting, Interative Services, News gathering and other broadband satellite applications (DVB-S2).

[5] Wilson, J. D.; Wintucky E. G.; Vaden, K. R.; Force, D. A.; Krainsky, I. L.; Simons, R. N.; Robbins, N. R.; Menninger, W. L.; Dibb, D. R. Lewis, D. E. , "Advances in Space Traveling-Wave Tubes for NASA Missions," Proc. IEEE, Special Issue on Technical Advances in Deep Space Communications & Tracking: Part I, vol. 95, no. 10, pp. 1958-1967, Oct. 2007.

[6] Sunde, E. D., "Intermodulation Distortion in Multicarrier FM Systems," IEEE International Convention, pp. 130-146, Mar. 1965.

[7] Shimbo, O., "Effects of Intermodulation, AM-PM Conversion, and Additive Noise in Multicarrier TWT Systems," Proc. IEEE, vol. 59, pp. 230-238, Feb. 1971.

[8] Rowe, H. E. "Memoryless Nonlinearities with Gaussian Inputs: Elementary Results," Bell Syst. Tech Journal, vol. 61, no. 7, pp 1520–1523, Sep. 1982.

[9] Minkoff, J., "The Role of AM-to-PM Conversion in Memoryless Nonlinear Systems," ," IEEE Trans on comm., vol. COM-33, no. 2, pp 139-144, Feb. 1985.

[10] Shaleh, A. A. M, "Frequency-Independent and Frequency-Dependent Nonlinear Model of TWT Amplifiers" IEEE Trans on comm., vol. 29, pp 1715-1720, 1981.

[11] Shannon, C. E., "Probability of Error for Optimal Codes in A Gassian Channel," Bell Syst. Tech. J., vol. 38, pp. 611-656, 1959.

[12] Feinstein, A., "A New Basic Theorem of Information Theory," IEEE Trans. Info. Theory, vol. 4., no.. 4, pp. 2-22, Sept 1954.

[13] Shannon, C. E., "Certain Results in Coding Theory for Noisy Channels," Inform. Contr., vol. 1, pp. 6-25, Sept 1957.

[14] Gallager, R. G., Information Theory and Reliable Comunication. New York, John Wiley & Sons, Inc. 1968.

[15] Laneman, J., "On the Distribution of Mutual Information," in Proc. Workshop on Information Theory and it's Applications. San Diego, CA, Feb. 2007.

[16] Verdú, S.; Han. T. S, "A General Formula for Channel Capacity," IEEE Trans. Info. Theory, vol. 40, pp 1147-1157, 1994.

[17] Polyanskiy, Y.; Poor, V.; Verdú, S.; "Channel Coding Rate in the Finite Blocklength Regime," IEEE Trans. Info. Theory, vol. 56, pp 2307-2358, 2010.

[18] Buckingham, D.; Valenti, M. C.; "The Information-Outage Probability of Finte-Length Codes over AWGN Channel," 42nd Annual Conf. Information Sciences and Systems, CISS, Mar. 2008.

[19] Bussgang, J. J., "Crosscorrelation Functions of Amplitude-Distorted Gaussian Signals," Research Lab. Electron, M.I.T. Tech Report No. 216, 1952.

[20] Gradshteyn, I. S; Ryzhik, I. M., Tables of Integrals, Series, and Products, 7th Ed., 2007.

[21] Spilker, J. J., Digital Communications by Satellite, Prentice Hall, 1st Edition, pp. 220-230, Feb. 1977.

Authorized licensed use limited to: Georgia Institute of Technology. Downloaded on January 12,2023 at 20:50:38 UTC from IEEE Xplore. Restrictions apply.